Inorg. Chem. **2008**, *47*, 154–161

Cobalt Coordination Induced Functionalized Molecular Clefts: Isolation of {Co^{III}–Zn^{II}} Heterometallic Complexes and Their Applications in Beckmann Rearrangement Reactions

Anurag Mishra,[†] Afsar Ali,[†] Shailesh Upreti,[‡] and Rajeev Gupta*,[†]

Department of Chemistry, University of Delhi, Delhi 110 007, India, and Department of Chemistry, Indian Institute of Technology—Delhi, New Delhi 110 016, India

Received August 20, 2007

The present work shows that the Co^{3+} coordination to the deprotonated pyridine-amide ligands orients the noncoordinated or *hanging* pyridine rings, thus furnishing a *cleft* in which Zn^{2+} ions coordinate. The building block approach points out a strategy to incorporate a Lewis acidic metal center in the periphery. This strategy has been used to synthesize Co^{3+}-centered–Zn^{2+}-peripheral heterobimetallic complexes. These heterobimetallic complexes have been thoroughly characterized including structural studies and have been successfully shown to catalyze the Beckmann rearrangement of the aldoximes and ketoxime to their respective amides.

Introduction

The importance of the pyridine-amide based ligands has always attracted the scientific community to explore their metallosupramolecular chemistry. This is mainly due to the ability of such ligands to cause self-assembly through coordinate bond formation (via pyridine) in conjunction with H-bonding (via amide C═O and N−H groups). Intriguing examples include Pd- and Pt-based molecular self-assemblies,[1] construction of Pd-based cages,[2] Ag- and Cd-based self-assembled two- and three-dimensional metallo-macrocycles,[3] d^{10}-metal clusters,[4] Zn-based self-assembled oligomers,[5] water−decamer stabilized Cu cluster,[6] self-assembled Pt-based nanoscopic rectangles,[7] and anion recognitionthrough hydrogen bonding in a Re-based system.[8] In all these examples, the judicious selection of the pyridine-amide based multidentate ligands with metal ions of the appropriate coordination geometry is quite apparent in controlling the dimensionality and topology of the resultant materials. Extending these fascinating studies, herein, we show the utilization of similar ligands to synthesize novel discrete heterobimetallic complexes where Co^{3+} coordination compounds are used as the building blocks. We also show the utilization of such heterobimetallic complexes in the Beckmann rearrangement reactions of the aldehyde- and ketone-oximes under mild reaction conditions. To the best of our knowledge, this is the first example of a heterometallic system catalyzed Beckmann rearrangement.

Results and Discussion

Design Aspects. The ligands HL^1 and H_2L^2 (Chart 1) have been chosen due to their unique ability to coordinate metal ions in a number of modes.[9] There are few possible modes of coordination of the ligands HL^1 and H_2L^2, and the case of ligand HL^1 is explained here. HL^1 may coordinate a metal center in three different modes: I, II, and III (Chart 1). Mode III can be ruled out as the current synthetic reaction involves

* To whom correspondence should be addressed. E-mail: rgupta@chemistry.du.ac.in.
[†] University of Delhi.
[‡] Indian Institute of Technology—Delhi.

(1) (a) Qin, Z.; Jennings, M. C.; Puddephatt, R. J. *Chem. Commun.* **2001**, 2676. (b) Qin, Z.; Jennings, M. C.; Puddephatt, R. J. *Chem. Commun.* **2002**, 354. (c) Qin, Z.; Jennings, M. C. Puddephatt, R. J. *Inorg. Chem.* **2003**, *42*, 1956.
(2) Noveron, J. C.; Lah, M. S.; Del Sesto, R. E.; Arif, A. M.; Miller, J. S.; Stang, P. J. *J. Am. Chem. Soc.* **2002**, *124*, 6613.
(3) Tzeng, B.-C.; Chen, B.-S.; Yeh, H.-T.; Lee, G.-H.; Peng, S.-M. *New J. Chem.* **2006**, *30*, 1087.
(4) Hou, H.; Wei, Y.; Song, Y.; Mi, L.; Tang, M.; Li, L.; Fan, Y. *Angew. Chem., Int. Ed.* **2005**, *44*, 6067.
(5) (a) Hunter, C. A.; Sarson, L. D. *Angew. Chem., Int. Ed. Engl.* **1994**, *33*, 2313. (b) Chi, X.; Guerin, A. J.; Haycock, R. A.; Hunter, C. A.; Sarson, L. D. *Chem. Commun.* **1995**, 2563. (c) Chi, X.; Guerin, A. J.; Haycock, R. A.; Hunter, C. A.; Sarson, L. D. *Chem. Commun.* **1995**, 2567.
(6) Barbour, L. J.; Orr, G. W.; Atwood, J. L. *Nature* **1998**, *393*, 671.
(7) Ghosh, S.; Mukherjee, P. S. *Dalton Trans.* **2007**, 2542.
(8) Sun, S.-S.; Lees, A. J. *Chem. Commun.* **2000**, 1687.
(9) (a) Perlepes, S. P.; Kabanos, T.; Hondrellis, V.; Tsangaris, J. M. *Inorg. Chim. Acta* **1988**, *150*, 13. (b) Dutta, S.; Bhattacharya, P. K.; Horn, E.; Tiekink, E. R. T. *Polyhedron* **2001**, *20*, 1815. (c) Singha, N. C.; Sathyanarayana, D. N. *J. Mol. Struct.* **1997**, *403*, 123. (d) Gudasi, K.; Vadavi, R.; Shenoy, R.; Patil, M.; Patil, S. A.; Nethaji, M. *Inorg. Chim. Acta* **2005**, *358*, 3799.

10.1021/ic7016424 CCC: $40.75
Published on Web 12/12/2007

Chart 1. Ligands Used and Their Coordination Modes

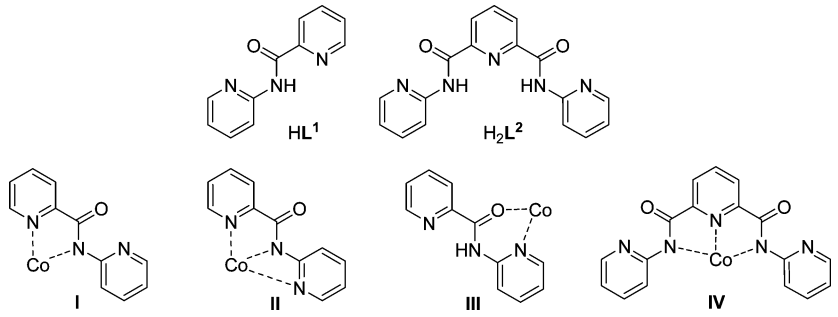

deprotonation of the ligand.[10] On the other hand, mode II can also be ruled out due to the geometric reason, as that would result in the formation of a strained four-membered chelate ring.[11] Arrangement I is the preferred mode of coordination via anionic amide-*N* and pyridine-*N* forming a five-membered chelate ring; however, it leaves the second pyridine ring of the ligand $[L^1]^-$ uncoordinated or *hanging*. Three uncoordinated or hanging pyridine rings would be available from an octahedral tris-ligated metal complex to interact with secondary metal ion(s). Moreover, the geometry of the central metal ion will dictate the orientation of the *molecular cleft* formed by the hanging pyridine rings.

The H_2L^2 ligand is an extension of the ligand HL^1. Here again coordination to the metal ion by the deprotonated form of the ligand is expected to leave two pyridine rings per ligand *hanging* (mode IV, Chart 1). Two of the hanging pyridine rings from two ligands may give rise to a *cleft*. However, in this case a bis-ligation is expected due to the tridentate nature of the ligand and two *clefts* per metal complex would be available to bind secondary metal ions.

Structures of $[Co(L^1)_3]$ (1) and $(ET_4N)[Co(L^2)_2]$ (2a). The compounds, $[Co(L^1)_3]$ (**1**) and $Na[Co(L^2)_2]$ (**2**) were synthesized following a recent report.[12] The molecular structure of complex **1** is shown in Figure 1 along with the important structural parameters (see Table S1, Supporting Information for complete bonding parameters). Three deprotonated ligands are arranged octahedrally around the Co^{III} ion via a five-membered chelate ring between amide-*N* and pyridyl-*N* atoms. The $Co-N_{amide}$ bond distances (average = 1.946 Å) are comparable to the $Co-N_{pyridine}$ bond distances (average = 1.944 Å), indicating a symmetrical bonding from all donors. All diagonal angles are more or less linear in nature, ranging from 174.5° to 176.0°, again suggesting a symmetrical arrangement of the donors resulting in a nearly octahedral geometry. Significant reduction of the bond angles from 90° involving the five-membered chelate rings was observed indicating a tight chelation; in fact, the average angle is only ~82.6°. The crystal structure of **1** clearly illustrates the *meridional* (*mer*) geometric isomeric form; as the dihedral angle between the coordinating planes comprising either three amide-*N* atoms [N(3), N(5), and N(6)] or three pyridyl-*N* atoms [N(1), N(2), and N(4)] is close to 180°.[13] The occurrence of the *mer* form has made all three ligands asymmetrical to each other, and this ligand asymmetry was observed in IR, ^1H, and ^{13}C NMR spectra with threefold peaks.[12]

For complex **2a**, there are two independent molecules in the unit cell besides two $(Et_4N)^+$ cations and a water molecule. The crystal structures of molecules **A** and **B** are shown in Figure 2 and S1, respectively. Both independent molecules (**A** and **B**, respectively) show certain differences in the bond lengths and bond angles. For molecule **B**, two water molecules (the second one is symmetrically generated) are present as a *diamond core* between two $[Co^{III}(L^2)_2]^-$ units (the second one is symmetrically generated) interacting terminally via hydrogen bonds to one oxygen atom of the amide group. The molecule **A** is unaltered; however, it has a quite unique orientation of the *hanging* pyridine rings. In fact, two of the hanging pyridine rings are in long-range interaction with the Co center (3.219 and 3.376 Å, respectively).[14] This weak interaction has altered the resonance structure of the connected amide group and resulted in a long bond to the Co ion (2.049 and 1.998 Å, respectively).

The Co(III) center is coordinated octahedrally by four deprotonated amide nitrogens in the equatorial plane and two pyridyl nitrogens in the axial positions. The ligand $[L^2]^{2-}$

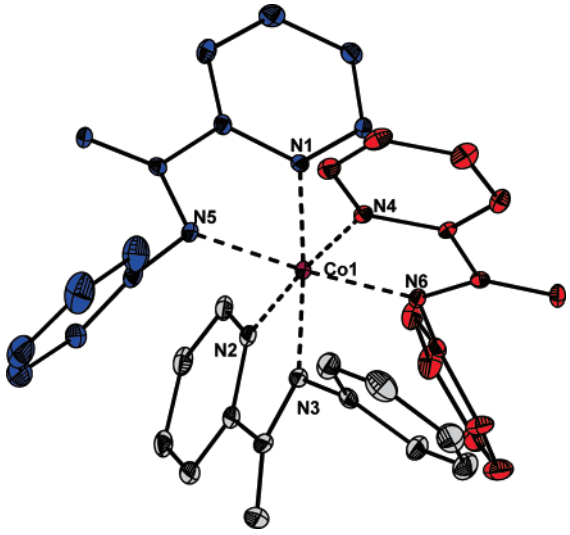

Figure 1. Thermal ellipsoidal representation (30% probability level with partial numbering scheme) of complex **1**. Hydrogen atoms and solvent molecule are omitted, while three ligands are shown in different colors for clarity. Selected bond lengths [Å] and angles [deg]: Co1−N1 1.958(3), Co1−N2 1.942(3), Co1−N3 1.946(3), Co1−N4 1.940(3), Co1−N5 1.957(3), Co1−N6 1.936(3); N1−Co1−N3 175.97(13), N2−Co1−N4 174.59(13), N5−Co1−N6 175.51(13).

(10) This type of coordination mode is suggested in literature; see ref 9a, for example.
(11) Hancock, R. D. *J. Chem. Educ.* **1992**, *69*, 615.
(12) Mishra, A.; Kaushik, N. K.; Verma, A. K.; Gupta, R. *Eur. J. Med. Chem.* **2007**, http://dx.doi.org/10.1016/j.ejmech.2007.08.015.

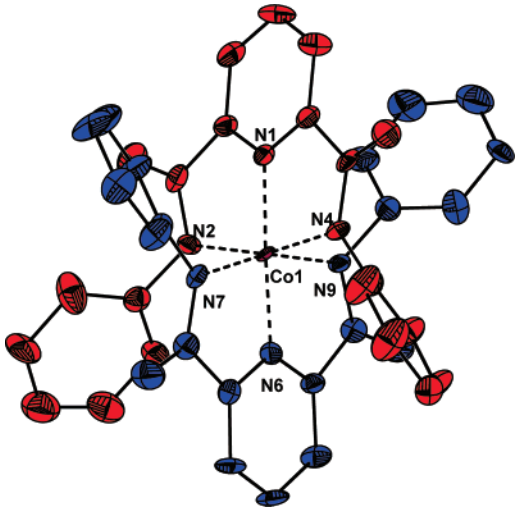

Figure 2. Thermal ellipsoidal representation (30% probability level with partial numbering scheme) of complex **2a** (molecules **A**; see Figure S1 for molecule **B**). Hydrogen atoms, cations, and solvent molecule are omitted, while two ligands are shown in different colors for clarity. Selected bond lengths [Å] and angles [deg]: Co1−N1 1.872(7), Co1−N2 1.998(7), Co1−N4 1.962(8), Co1−N6 1.870(7), Co1−N7 1.935(8), Co1−N9 2.048(7); N1−Co1−N6 175.2(3), N2−Co1−N4 162.8(3), N7−Co1−N9 162.4(3).

coordinates in a meridional fashion as observed before for the Co^{III} complex of a closely similar ligand (2,6-bis(*N*-phenylcarbamoyl)pyridine).[15,16] The geometry around the cobalt center can best be described as compressed octahedral with significant deviation from 90° of the bond angles.[15,16] The average $M-N_{amide}$ and $M-N_{pyridine}$ bond lengths are slightly on the longer and shorter side, respectively, as noted before.[15,16] In each ligand the two *N*-pyridine rings make angles of varying degrees with each other and they also make significant angles with the central pyridine ring. This points out that the hanging pyridine rings are poorly preorganized in the absence of the secondary metal ion (cf. Crystal Structure of **4a**). The five-membered chelate rings are more or less planar to each other, with the deviation being less than 2° for molecule **A** while a somewhat distorted arrangement was noticed for molecule **B** with the dihedral angle between the chelate planes reaching the value of ∼5°.

Interestingly, the coordination mode of the ligands, $[L^1]^-$ and $[L^2]^{2-}$, leaves one or two of the pyridine rings uncoordinated or hanging; three (one from each bidentate ligand) and four (two from each tridentate ligand) pyridine rings

Scheme 1. Synthesis of Complex **3**

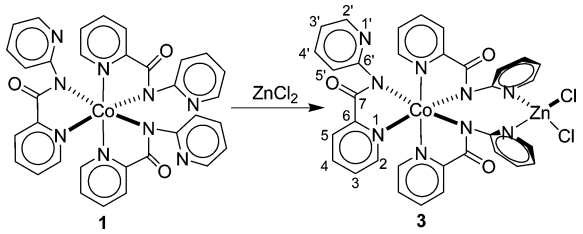

Scheme 2. Syntheses of Complexes **4**, **4a**, and **4b**

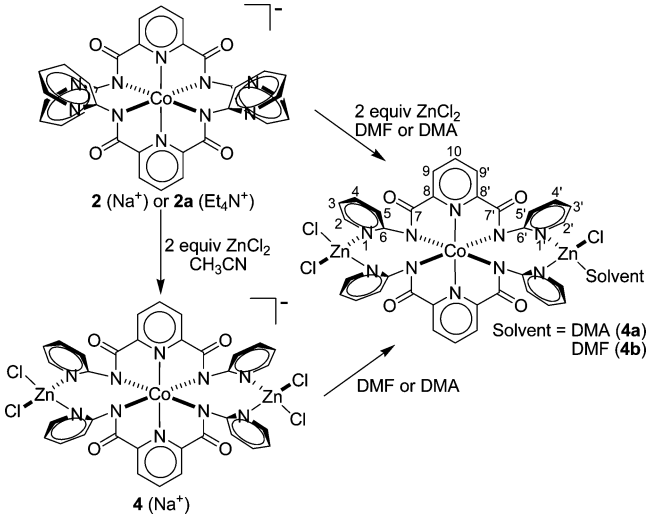

remain uncoordinated from complexes **1** and **2**, respectively. Two of these hanging pyridine rings converge to form a cleft that coordinates to the Zn^{2+} ion(s) (vide infra).

Reaction of $[Co(L^1)_3]$ (1) with $ZnCl_2$: Isolation of $[1-ZnCl_2]$ (3). The reaction between the complex **1** and $ZnCl_2$ afforded the complex **3** as deep-red blocks (Scheme 1). Notably, the coordination of the hanging pyridine rings to the $ZnCl_2$ resulted in a visible color change from brown to deep red (Figure S2). Complex **3** behaved as a nonelectrolyte in organic solvents such as dimethylformamide (DMF) and dimethyl sulfoxide (DMSO); however, in water it behaved as a 1:1 electrolyte.[17] We suspect that partial hydrolysis of the complex takes place in water to give a $[Co^{III}(L^1)_3-Zn(Cl)]^+$ species. The same species was observed as a molecular ion (m/z = 754.3462) in the mass spectrum of complex **3** (recorded in water). Three distinct $C{=}O_{amide}$ stretches were observed at 1635, 1600, and 1565 cm^{-1} as also noted for **1**.[12] The slight shifts in the values from complex **1** indicate the differences arising in the resonance structures of the amide group due to hanging versus coordinated nature of the pyridine rings.

Reaction of $Na[Co(L^2)_2]$ (2) with $ZnCl_2$: Isolation of $Na[2-(ZnCl_2)_2]$ (4). Complex **4** was synthesized (Scheme 2) in a manner similar to that of **3** and again resulted in a visible color change from deep green to yellowish brown (Figure S2). The integrity of the complex in the solution state was confirmed by recording the mass spectrum in DMSO, where a peak was obtained at 895.3060 that corresponds to $\{[Co(L^2)_2-(ZnCl)_2]^+\}$ species. Conductivity measurements[17]

(13) The two planes comprising all three amide-*N* atoms and all three pyridine-*N* atoms make an angle of ∼85° with each other.

(14) The analogous distances for molecule **B** are in the range 3.350−3.637 Å. Similar types of long-range interactions (3.50−3.72 Å) are reported for a Co(III) complex of a closely similar ligand; see: Bricks, J. L.; Reck, G.; Rurack, K.; Schulz, B.; Spieless, M. *Supramol. Chem.* **2003**, *15*, 189.

(15) Ray, M.; Ghosh, D.; Shirin, Z.; Mukherjee, R. *Inorg. Chem.* **1997**, *36*, 3568.

(16) Mukherjee and co-workers have used the ligand, 2,6-bis(*N*-phenylcarbamoyl)pyridine to synthesize a family of structurally characterized octahedral metal complexes with $M^{III}N_6$ coordination. In all these cases compressed octahedral geometry with short $M-N_{pyridine}$ and long $M-N_{amide}$ bond distances was observed. The authors have explained this unusual trend due to the result of steric predominance over electronic effects. Our results for the complex **2a** corroborate the findings of Mukherjee and co-workers. See: (a) Reference 15. (b) Patra, A. K.; Mukherjee, R. *Inorg. Chem.* **1999**, *38*, 1388. (c) Singh, A. K.; Balamurugan, V.; Mukherjee, R. *Inorg. Chem.* **2003**, *42*, 6497.

(17) Geary, W. J. *Coord. Chem. Rev.* **1971**, *7*, 81.

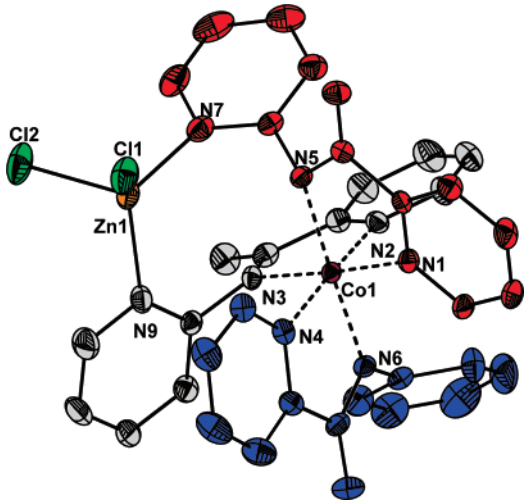

Figure 3. Thermal ellipsoidal representation (30% probability level with partial numbering scheme) of complex **3**. Hydrogen atoms and solvent molecule are omitted, while three ligands are shown in different colors for clarity. Selected bond lengths [Å] and angles [deg]: Co1−N1 1.963(4), Co1−N2 1.935(5), Co1−N3 1.931(4), Co1−N4 1.949(4), Co1−N5 1.989(4), Co1−N6 1.946(4), Zn1−N7 2.024(5), Zn1−N9 2.048(5), Zn1−Cl1 2.2311(19), Zn1−Cl2 2.2525(19); N1−Co1−N3 175.64(18), N2−Co1−N4 173.89(19), N5−Co1−N6 177.02(18), N7−Zn1−N9 110.9(2), Cl1−Zn1−Cl2 108.25(7).

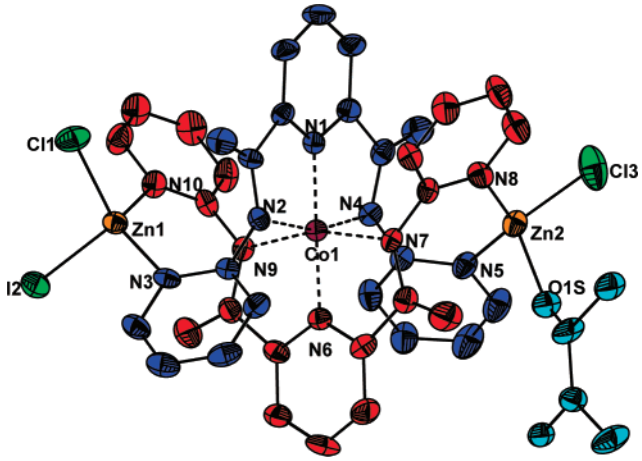

Figure 4. Thermal ellipsoidal representation (30% probability level with partial numbering scheme) of complex **4a**. Hydrogen atoms and solvent molecules are omitted, while two ligands are shown in different colors for clarity. Coordinated DMA is shown in cyan color. Selected bond lengths [Å] and angles [deg]: Co1−N1 1.867(7), Co1−N2 1.970(7), Co1−N4 1.951(7), Co1−N6 1.877(7), Co1−N7 1.970(7), Co1−N9 1.955(7), Zn1−N3 2.065(8), Zn2−N5 2.017(8), Zn2−N8 2.040(8), Zn1−N10 2.062(8), Zn1−Cl1 2.243(3), Zn1−Cl2 2.251(3), Zn2−Cl3 2.210(4), Zn2−O1S 1.946(12); N1−Co1−N6 177.1(3), N2−Co1−N4 162.3(3), N7−Co1−N9 162.5(3), N3−Zn1−N10 122.1(3), Cl1−Zn1−Cl2 108.05(12), N5−Zn2−N8 127.3(3), O1S−Zn2−Cl3 110.2(5).

in solvents such as DMF and *N*,*N*′-dimethylacetamide (DMA) indicate partial replacement of the bound Cl^- ion by the solvent as noted before for complex **3**; in fact, two new complexes **4a** and **4b** were isolated (see next section).

Recystallization from DMA or DMF: Isolation of [2−($ZnCl_2$)(Zn(Cl)(DMA)] (4a) or [2−($ZnCl_2$)(Zn(Cl)-(DMF)] (4b). When complex **4** was recrystallized from *N*,*N*′-dimethylacetamide (DMA), interestingly, a new compound, **4a**, was isolated and structurally characterized (vide infra). The crystal structure shows that one of the chloride ions is replaced by the solvent DMA to afford the neutral compound **4a**. It is worth mentioning here that complex **4**, i.e., Na[2−($ZnCl_2$)$_2$], is quite stable in the solid state as well as in CH_3CN; however, during recrystallization from DMA one Cl^- was replaced by the solvent. A similar observation was noticed in DMF, and an analogous DMF-coordinated complex, **4b**, was isolated. It is likely that a better coordinating solvent such as DMA or DMF has the ability to replace Cl^- ion than a poor coordinating solvent such as CH_3CN. The complexes **4a** and **4b**, as expected, are nonconducting, display characteristic peaks for the coordinated DMA and DMF in the FTIR and ^{1}H NMR spectra,[18] and show distinct thermal behavior (vide infra).

Crystal Structure of 3. The structure of **3** shows that the Zn^{2+} ion coordinates to two of the hanging pyridine rings emerging from the central octahedral Co^{3+} core (Figure 3). The remaining two coordinations come from the Cl^- groups completing the tetrahedral geometry around the Zn^{2+} ion. The Co−N_{amide} (average = 1.955 Å) and Co−$N_{pyridine}$ (average = 1.949 Å) bond distances are marginally longer than those in **1**. However, one of the Co−N_{amide} bond distances at 1.989 Å is much longer than the others, suggesting that the pyridine ring attached to this amide group has stretched out to make room for the Zn^{2+} ion. The third hanging pyridine remains uncoordinated. The average angle for the five-membered chelate rings is ∼82.4°, which is comparable to that of **1** and suggests that the coordination of the Zn ion in the *cleft* has not caused much distortion to the chelate structure of the central Co ion. The angles between the five-membered chelate plane and the plane of hanging pyridine ring are comparable to that of complex **1**. However, the uncoordinated hanging pyridine ring is much more out of plane (making an angle of ∼74° with the five-membered chelate plane) than the rings that are coordinated to the Zn ion (making angles of ∼67° and ∼70° with the five-membered chelate plane, respectively).

Crystal Structure of 4a. The molecular structure of complex **4a** along with the selected bonding parameters is shown in Figure 4. Two Zn^{2+} ions are situated in two clefts created by the hanging pyridine rings originating from the central cobalt core. Zn1 is externally coordinated by two Cl^- groups, whereas Zn2 has one Cl^- and one DMA molecule. The average Zn1−$N_{pyridine}$ distance of 2.064 Å is quite longer than in **3** (2.036 Å), while the similar distance for Zn2 at 2.029 Å is little shorter. This is most likely due to the difference in the number of anionic ligands attached to two Zn centers. A similar observation is noted for the respective Zn−Cl distances. The average Zn1−Cl distance of 2.247 Å is much longer than the Zn2−Cl3 distance of 2.210 Å, but comparable to that in **3** (2.242 Å). The geometry around the central Co^{3+} ion is distorted octahedral as noted for its precursor **2a**. The average Co−$N_{pyridine}$ (1.872 Å) and Co−N_{amide} (1.962 Å) distances are quite similar to those in **2a**. The two pyridine rings are trans to each other and make an angle of ∼177° with the Co ion. The distorted N_4 basal plane composed of N_{amide} groups perfectly housed the Co ion. The

(18) The ^{1}H signals due to coordinated DMA (DMF) molecule were noticed at 1.98, 2.81, and 2.97 (2.77, 2.94, and 7.96) ppm.

average $Co-N_{pyridine}$ distance of 1.872 Å is quite similar to those observed for molecules **A** and **B** (1.871 and 1.870 Å, respectively) of complex **2a**. In addition, the average $Co-N_{amide}$ distance of 1.962 Å is closer to that in molecule **B** (1.966 Å); however, it is marginally longer than that in molecule **A** (1.986 Å). The five-membered chelate rings are almost planar to each other, making an angle of ~2° as observed before for molecule **A** of **2a**. Finally, the central pyridine ring of each ligand makes an angle in the range of 70−85° with the pyridine rings coordinated to the Zn ions.

The cleft effect can be evaluated by comparing **3** and **4a** with the reported structure of $[Zn(py)_2(Cl)_2]$ (**5**)[19] having the partial structure of heterobimetallic complexes. The average $Zn-N_{pyridine}$ distances for **3** and **4a** are quite comparable to those in **5** (2.049 Å); however, the Zn−Cl distances are marginally longer than those in **5** (2.2215 Å). The longer Zn−Cl distances in **3** and **4a** than in **5** suggest a better Lewis acidic nature of the zinc ion in the former cases. The *cleft effect* on the geometry of the Zn^{2+} ion in complexes **3** and **4a** is quite significant. For example, the N−Zn−N angle is 110.9° for **3**, ~4° bigger than **5**; however, increases of ~16° and 21° were observed for Zn1 and Zn2 centers, respectively, for **4a**. This trend indicates that hanging pyridine rings are much more twisted in **4a** than in **3**, possibly to accommodate two zinc ions in the former case. Similarly, the Cl−Zn−Cl angle has been reduced by ~13° in **3** compared to **5**; an almost identical reduction was observed for the Zn1 center in **4a**. In essence, the reduction of the Cl−Zn−Cl angle is being compensated by the enlargement of the N−Zn−N angle for **3** and **4a** and suggests that pyridine rings are twisted to make room to accommodate the Zn^{2+} ion(s).

NMR Studies. The ^1H and ^{13}C NMR spectra of complex **3** are very similar to those of **1** (Figure S3).[12] This is not completely unexpected as coordination to a diamagnetic Zn center may not have significantly altered the chemical environment of the protons or carbons. However, it is to be noted that a few proton signals become quite broad, and we tentatively assign them as the pyridine-H closer to the Zn center. The ^1H NMR spectrum of $[\mathbf{2}-(ZnCl_2)_2]$ (**4**) was also much broader in general, and a number of signals were merged. The proton NMR spectrum (Figure S4) of **4a** is quite different from that of **4** and clearly shows the signals due to coordinated DMA molecule. Moreover, a downfield shift of 0.2 ppm was observed for the H_2 and $H_{2'}$ protons. This shift is, most likely, due to the enhanced electron density requirement at the Zn center after the replacement of an anionic ligand, Cl^-, by a neutral ligand, DMA. This effect is more pronounced for the H_2 and $H_{2'}$ protons than for the rest of the *N*-pyridine protons. Finally, the ^{13}C NMR spectra of **4** and **4a** are quite similar to each other except for the coordinated DMA.

Complexes **4a** and **4b** have also been used for the catalytic reaction in DMF at 100 °C (vide infra). In order to obtain information about the solution state structure and stability of these complexes at elevated temperature, their ^1H NMR spectra were recorded in DMF-d_7 at three different temperatures: 30, 50, and 100 °C (Figures S5 and S6). The results indicate that both complexes **4a** and **4b** maintain their structure at all three temperatures of study.

Thermal Analyses. The complexes **4a** and **4b** were further examined by thermogravimetric analysis (TGA) and differential thermal analysis (DTA) to gain insight into the nature of the coordinated solvent molecule (DMA or DMF). The overall thermal profiles of both complexes are quite similar (Figure S7). For example, both **4a** and **4b** show a broad endothermal feature in the temperature range of ~50 °C which we tentatively assign as the loss of water molecule present as solvent of crystallization. TGA showed that this event corresponded to a ~2−3% weight loss from the sample and fits well with experimentally observed value of ~1.7% for one water molecule. This is followed by a sharp endothermic feature centered at ~125 °C for **4a** and ~100 °C for **4b** which we assign as the loss of the coordinated DMA for the former and DMF for the later. The experimental weight loss of ~5−6% matches nicely with calculated loss for one DMA or DMF molecule in the range of ~7−8%. The difference of ~25 °C between the two complexes can be correlated with the boiling point difference of the two solvents (boiling points of DMF and DMA are 153 and 165 °C, respectively). The thermal analysis findings are well supported by the elemental analyses and NMR spectral data for complexes **4a** and **4b**.

Organic Transformations. The presence of the exposed Lewis acidic metal ions, Zn^{2+}, in our heterobimetallic complexes, prompted us to explore organic transformation reactions. Very few examples are available in the literature to utilize a well-characterized supramolecular or heterometallic system for the organic transformation. Fujita[20] has shown Cd^{2+}−4,4′-bpy coordination network mediated cyanosilylation reactions where the Lewis acidic Cd^{2+} ion activates the substrate. Other intriguing examples include the application of metal−organic frameworks (MOFs) for the enolization and Aldol reactions,[21] Diels−Alder reaction,[22] and enantioselective separation.[23] Very recently, heterobimetallic porphyrin pincer complexes were shown to catalyze the Heck reaction where the central metal ion (Ni, Cu, and Zn) significantly influences the activity of the peripheral and catalytic Pd center.[24]

The transformation we selected is the Beckmann rearrangement (BR), a commercially and industrially important reaction that is known to be catalyzed by the participation of a Lewis acid. The BR generally requires a high reaction temperature, a strong acidic and dehydrating medium, and, thus, leads to several byproducts and is not suitable for sensitive substrates.[25] Several catalysts[26] such as sulfamic acid, chlorosulfonic acid, sulfonyl chloride, PCl_5, BF_3,

(19) Steffen, W. L.; Palenik, G. J. *Acta. Crystallogr.* **1976**, *B32*, 298.

(20) (a) Ohmori, O.; Fujita, M. *Chem. Commun.* **2004**, 1586. (b) Fujita, M.; Kwon, Y. J.; Washizu, S.; Ogura, K. *J. Am. Chem. Soc.* **1994**, *116*, 1151.

(21) Dewa, T.; Saiki, T.; Aoyama, Y. *J. Am. Chem. Soc.* **2001**, *123*, 502.

(22) Endo, K.; Koike, T.; Sawaki, T.; Hayashida, O.; Masuda, H.; Aoyama, Y. *J. Am. Chem. Soc.* **1997**, *119*, 4117.

(23) Evans, O. R.; Ngo, H. L.; Lin, W. *J. Am. Chem. Soc.* **2001**, *123*, 10395.

(24) Yamaguchi, S.; Katoh, T.; Shinokubo, H.; Osuka, A. *J. Am. Chem. Soc.* **2007**, *129*, 6392.

Table 1. Crystallographic and Structural Refinement Data for **1**·DMF, **2a**·H_2O, **3**·CH_3CN, and **4a**·2DMA

	1·DMF	**2a**·H_2O	**3**·CH_3CN	**4a**·2DMA
molecular formula	$C_{33}H_{24}CoN_9 \cdot C_3H_7NO$	$(C_{34}H_{22}CoN_{10}O_4)_2(C_8H_{20}N)_2 \cdot H_2O$	$(C_{33}H_{24}Cl_2CoN_9O_3Zn)_2 \cdot C_2H_3N$	$C_{38}H_{31}Cl_3CoN_{11}O_5Zn_2 \cdot (C_4H_9NO)_2$
fw	726.64	1665.59	1620.72	1192.04
T (K)	100	298	298	298
crystal system	monoclinic	monoclinic	monoclinic	monoclinic
space group	$P2_1/n$	$P2_1/n$	$C2/c$	$P2_1/c$
a (Å)	8.808(5)	19.423(9)	31.283(3)	17.608(4)
b (Å)	14.788(5)	22.614(11)	14.2505(13)	18.924(5)
c (Å)	25.216(5)	19.882(10)	22.139(2)	16.472(4)
β (°)	90.567(5)	111.393(12)	129.8370(10)	108.498(5)
V (Å$_3$)	3284(2)	8131(7)	7578.5(12)	5205(2)
Z	4	4	4	4
d (g cm^{-3})	1.470	1.359	1.421	1.521
F(000)	1504	3472	3288	2440
goodness of fit (F^2)	1.207	1.277	1.194	0.992
R_1, wR_2 [$I > 2\sigma(I)$]	0.0750, 0.1792	0.0713, 0.1423	0.0784, 0.2082	0.0527, 0.1669
R_1, wR_2 (all data)[a]	0.1155, 0.1946	0.0835, 0.1524	0.0930, 0.2225	0.0745, 0.1881

[a] $R_1 = \sum||F_o| - |F_c||/\sum|F_o|$; $wR = \{[\sum(|F_o|^2|F_c|^2)^2]\}^{1/2}$.

cyanuric chloride, metal salts, metal oxides, clays, zeolites, and ionic liquids have been employed for the BR. The majority of these reactions were attempted as conventional liquid-phase reactions, while a few of them focused on vapor-phase processes. Solvent-free microwave-assisted rearrangement has also been attempted.[27] Several cocatalysts have also been used in conjunction with the catalyst to improve the activity.[26c] $ZnCl_2$ was found to be the most effective cocatalyst in the majority of these literature precedents.[26c,g,t] The presence of the $ZnCl_2$ fragment(s) in our heterometallic complexes **3**, **4**, **4a**, and **4b** immediately suggested their potential application. A variety of aldoximes and ketoximes were tested, and the results are presented in Table 2. Aldoximes gave only the primary amides and did not show any traces of the nitriles and aldehydes which are the commonly observed byproducts[25] (entries 1−6). The BR is generally suggested to proceed through *anti* migration, wherein the *Z*-forms of the oximes are expected to give the corresponding amides.[26k] In the case of unsymmetrical ketoximes, the reaction was found to be selective and only one of the two possible amides was produced[27b] (entries 7−10). For alkyl aryl ketoxime, it is generally the aryl group that preferentially migrates, as noted here[25a] (entries 7−10). The introduction of the electron-releasing group at the para position of the migrating aryl group in alkyl aryl ketoxime resulted in a better yield as the rearrangement is likely to be accelerated (entries 8−10). A similar trend was noticed for the aldoximes (entries 2−4). The meta-substituted aldoxime gave a poorer yield than the ortho- or para-substituted cases (entries 4−6). The catalyst **4a** was also shown to have similar results (entries 11 and 12) and suggests that the coordinated solvent does not play any significant role in the reaction except for providing the labile site.

Complexes **4a** and **4b** were found to be the most efficient catalysts, whereas **3** and **4** only poorly promoted the reaction (entries 13, 14, 17, and 18), while $ZnCl_2$[28] and $[(py)_2ZnCl_2]$**5** were almost ineffective (entries 19 and 20). This is to be noted, however, complex **4** also catalyzed the BR when the reaction was carried out in DMF as that would in-situ generate the catalyst **4b** (entries 15 and 16). The inability of the complexes **3**, **4**, and **5** to promote BR strongly indicates that the labile site is essential for the observed catalytic activity. We believe that the coordinated solvent molecule (DMA in **4a** and DMF in **4b**) is first replaced by the oxime in the initiation step. This speculation is further supported by the fact that the ketoxime with sterically demanding substituents, such as benzophenone-oxime, did not give any BR products, as the substrate was, probably, unable to approach the Zn center. Most importantly, catalysts **4a** and **4b** can be isolated after the reaction and reused (tested eight times) without a significant drop in the catalytic performance (entries 21 and 22). Finally, the Cd^{2+} analogue of **4b** did not show the BR reaction under similar reaction conditions,[29] thus confirming the uniqueness of the Zn^{2+} ions in hetero-

(25) (a) Smith, M. B.; March, J. In *Advanced Organic Chemistry*, 5th ed.; John Wiley & Sons: New York, 2001; p 1415 and references therein. (b) Maruoka, K.; Yamamoto, H. In *Comprehensive Organic Synthesis*; Pergamon Press: Oxford, 1991; Vol. 6, pp 763−765 and references therein.

(26) Sulfamic acid, PCl_5: (a) Wang, B.; Gu, Y.; Luo, C.; Yang, T.; Yang, L.; Suo, J. *Tetrahedron Lett.* **2004**, *45*, 3369. (b) Gui, J.; Deng, Y.; Hu, Z.; Sun, Z. *Tetrahedron Lett.* **2004**, *45*, 2681. P_2O_5: (c) Sato, H.; Yoshioka, H.; Izumi, Y. *J. Mol. Catal., A: Chem.* **1999**, *149*, 25. Metal salts: (d) De, S. K. *J. Chem. Res.* **2004**, 131. (e) De, S. K. *Synth. Commun.* **2004**, *34*, 3431. BF_3: (f) Anilkumar, R.; Chandrasekhar, S. *Tetrahedron Lett.* **2000**, *41*, 5427. Cyanuric chloride: (g) Furuya, Y.; Ishihara, K.; Yamamoto, H. *J. Am. Chem. Soc.* **2005**, *127*, 11240. (h) De Luca, L.; Giacomelli, G.; Porcheddu, A. *J. Org. Chem.* **2002**, *67*, 6272. PCl_5, sulfonyl chloride, chlorosulfonic acid: (i) Li, D.; Shi, F.; Guo, S.; Deng, Y. *Tetrahedron Lett.* **2005**, *46*, 671. (j) Peng, J.; Deng, Y.; *Tetrahedron Lett.* **2001**, *42*, 403. ZnO: (k) Sharghi, H.; Hosseini, M. *Synthesis* **2002**, 1057. Supported oxides: (l) Dongare, M. K.; Bhagwat, V. V.; Ramana, C. V.; Gurjar, M. K. *Tetrahedron Lett.* **2004**, *45*, 4759. (m) Mao, D.; Chen, Q. Lu, G. *Appl. Catal., A: Gen.* **2003**, *244*, 273. Zeolites: (n) Maheswari, R.; Sivakumar, K.; Sankarasubbier, T.; Narayanan, S. *Appl. Catal., A: Gen.* **2003**, *248*, 291. (o) Chaudhuri, K.; Bal, R.; Chandwadkar, A. J.; Sivasanker, S. *J. Mol. Catal. A: Chem.* **2002**, *177*, 247. (p) Dahlhoff, G.; Barsnick, U.; Holderich, W. F. *Appl. Catal., A: Gen.* **2001**, *210*, 83. (q) Tsai, C. C.; Zhong, C. Y.; Wang, I.; Liu, S. B.; Chen, W. H.; Tsai, T. C. *Appl. Catal., A: Gen.* **2004**, *267*, 87. (r) Thomas, J. M.; Raja, R. *Prroc. Natl. Acad. Sci. U.S.A.* **2005**, *102*, 13732. Ionic liquids: (s) Ren, R. X.; Zueva, L. D.; Ou, W. *Tetrahedron Lett.* **2001**, *42*, 8441. BOP-Cl: (t) Zhu, M.; Cha, C.; Deng, W.-P.; Shi, X.-X. *Tetrahedron Lett.* **2006**, *47*, 4861.

(27) (a) Loupy, A.; Regnier, S. *Tetrahedron Lett.* **1999**, *40*, 6221. (b) Li, Z.; Ding, R.; Lu, Z.; Xiao, S. Ma, X. *J. Mol. Catal. A: Chem.* **2006**, *250*, 100.

(28) Thus also ruling out the involvement of free $ZnCl_2$ in catalytic reaction that may have generated from **4a** or **4b** under the reaction conditions.

(29) Mishra, A.; Gupta, R. Unpublished results.

Table 2. Beckmann Rearrangement Reaction Catalyzed by **3**, **4**, **4a**, and **4b** in DMF at 100 °C, 5 mol % Catalyst, and Reaction Time of 2 h

entry	catalyst	R_1	R_2	yield,[a] TON[b]
1	**4b**	H	Ph	60, 12
2	**4b**	H	*p*-(MeO)C_6H_4	65, 13
3	**4b**	H	*p*-(Cl)C_6H_4	45, 9
4	**4b**	H	*p*-(NO_2)C_6H_4	40, 8
5	**4b**	H	*o*-(NO_2)C_6H_4	30, 6
6	**4b**	H	*m*-(NO_2)C_6H_4	10, 2
7	**4b**	Ph	CH_3	58, 12
8	**4b**	*p*-(MeO)C_6H_4	CH_3	60, 12
9	**4b**	*p*-(Cl)C_6H_4	CH_3	35, 7
10	**4b**	*p*-(NO_2)C_6H_4	CH_3	30, 6
11	**4a**	H	Ph	63, 13 (65, 13)[c]
12	**4a**	Ph	CH_3	60, 12 (60, 12)[c]
13	**4**[d]	H	Ph	10, 2
14	**4**[d]	Ph	CH_3	8, 2
15	**4**	H	Ph	56, 11
16	**4**	Ph	CH_3	58, 12
17	**3**	H	Ph	6, −
18	**3**	Ph	CH_3	7, −
19	**5**	Ph	CH_3	5, −
20	$ZnCl_2$	Ph	CH_3	5, −
21	**4a**[e]	Ph	CH_3	55, 11 (first run), 53, 11 (second run), 48, 10 (eighth run)
22	**4b**[c,e]	Ph	CH_3	58, 12 (first run), 56, 11 (second run), 50, 10 (eighth run)

[a] Isolated yield. [b] TON, turnover number = no. of moles of product/no. of moles of catalyst. [c] The reaction was done in DMA. [d] The reaction was performed in CH_3CN. [e] The reused catalyst was employed in the reaction.

bimetallic complexes **4a** and **4b** for the observed catalytic BR reactivity.

Conclusions

In summary, we have shown a novel method to synthesize Co-centered−Zn-peripheral heterobimetallic complexes where coordination compounds are used as the building blocks. Our strategy utilizes the design of the ligand to selectively coordinate a central metal ion while leaving an auxiliary group to afford a preorganized molecular cleft to bind a secondary metal ion. Also demonstrated is a unique way to restrict the dimensionality of the building blocks to afford discrete complexes. The crystal structures of the heterobimetallic complexes show that the Lewis acidic Zn^{2+} ion (ions) is (are) attached to the cleft created by the *hanging* pyridine rings. We also show, for the first time, heterometallic complex catalyzed Beckmann rearrangement. Our results suggest that the labile site (sites) is (are) required for the BR reaction. Further studies are in progress to increase the number of labile sites on the peripheral Zn centers to improve the efficiency of the catalyst and to explore the effect of the central metal ion on the catalytic performance of the system.

Experimental Section

Syntheses. The ligands HL^1 and H_2L^2 were synthesized according to the published procedures.[30] The complexes **1** and **2** were synthesized according to our recent report.[12] Aldehyde- and ketone-oximes were prepared by the standard procedures, whereas the respective amide products were characterized by comparison of their melting points, IR spectra, and ^1H NMR spectra with those of authentic samples.

Synthesis of $(Et_4N)[Co(L^2)_2]$ (2a). The ligand H_2L^2 (1.0 g, 3.10 mmol) was dissolved in CH_2Cl_2 (50 cm^3), and to it was added $Co(OAc)_2{\cdot}4H_2O$ (0.39 g, 1.56 mmol) and K_2CO_3 (10.78 g, 77.9 mmol). The mixture was subsequently heated at reflux for 4 h. To the resulting deep-red solution, solid $Et_4NCl{\cdot}xH_2O$ (1.02 g, 6.2 mmol) was added and stirred for 2 h at room temperature; exposure to air resulted in a deep-green solution. Removal of the solvent was followed by addition of DMF and filtration. On concentration and addition of diethyl ether a dark precipitate resulted. Recrystallization from DMF−Et_2O (vapor diffusion) afforded a crystalline solid suitable for structural studies. Yield: 0.53 g (42%). Anal. Calcd for $C_{42}H_{44}N_{11}O_5Co{\cdot}H_2O$: C, 59.92; H, 5.27; N, 18.30. Found: C, 59.63; H, 5.50; N, 18.41. IR (KBr, selected peaks, C═O): 1615, 1576, 1560 cm^{-1}. Conductivity (DMF, ∼1 mM solution at 298 K): $\Lambda_M = 65\ \Omega^{-1}\ cm^2\ mol^{-1}$. Absorption spectra [$\lambda_{max}$, nm, DMF ($\epsilon$, $M^{-1}\ cm^{-1}$)]: 650 (200), 470 (sh, 2100), 435 (sh, 3150), 385 (8500), 328 nm (18 000). ES-MS (CH_3OH, *m*/*z*): Obsd 694.0164 (100) [{[$Co(L^2)_2$] + H^+}$^+$]; Calcd 694.13. ^1H NMR [DMSO-d_6, 300 MHz]: δ = 7.40 (d, 4H, $H_2/H_{2'}$), 6.45 (m, 4H, $H_3/H_{3'}$), 7.04 (m, 4H, $H_4/H_{4'}$), 7.30 (d, 4H, $H_5/H_{5'}$), 6.78 (d, 4H, $H_9/H_{9'}$), 7.74 (t, 2H, H_{10}), 2.94 (−CH_2−, Et_4N^+), 0.90 (−CH_3, Et_4N^+). ^{13}C NMR [DMSO-d_6, 300 MHz]: δ = 7.06 (−*C*H_3, Et_4N^+), 51.39 (−*C*H_2−, Et_4N^+), 147.26 (C_2), 122.24 (C_3), 122.84 (C_4), 117.92 (C_5), 157.14 (C_6), 167.45 (C_7), 159.64 (C_8), 135.45 (C_9), 138.60 (C_{10}).

Synthesis of $[Co(L^1)_3{-}ZnCl_2]$ (3). A solution of $ZnCl_2$ (0.065 g, 0.470 mmol) in CH_3CN (2 cm^3) was added to a solution of complex **1** (0.100 g, 0.153 mmol) in CH_3CN (2 cm^3). The resultant deep-red solution was stirred for 1 h. The vapor diffusion of diethyl ether to the filtrate afforded deep-red crystalline product within a day. This product was filtered and air-dried. Yield: 0.110 g (91%). Anal. Calcd for $C_{33}H_{26}N_9O_4Cl_2CoZn{\cdot}H_2O$: C, 49.06; H, 3.24; N, 15.60. Found: C, 48.80; H, 3.38; N, 16.06. IR (KBr, selected peaks,

(30) See refs 9a and 9b for HL^1, and: (a) Jain, S. L.; Bhattacharyya, P.; Milton, H. L.; Slawin, A. M. Z.; Crayston, J. A. Woolins, J. D. *Dalton Trans.* **2004**, 862; (b) Hou, H.; Wei, Y.; Song, Y.; Mi. L.; Tang, M.; Li, L.; Fan, Y. *Angew. Chem., Int. Ed.* **2005**, *44*, 6067 for H_2L^2.

C═O): 1635, 1600, 1565 cm^{-1}. Conductivity (~1 mM solution at 298 K): Λ_M = 10 (in DMSO), 250 (in H_2O) Ω^{-1} cm^2 mol^{-1}. Absorption spectra [$\lambda_{max,}$ nm, CH_3CN (ϵ, M^{-1} cm^{-1})]: 512 (220), 377 (sh, 4300), 303 nm (21 000). ES-MS (H_2O, *m*/*z*): Obsd 754.3462 (60) [{$Co(L^1)_3(ZnCl)$}$^+$], 717.35 (80) [{$Co(L^1)_3(Zn)$}$^{2+}$ + H^+]. ^{1}H NMR [DMSO-d_6, 300 MHz]: δ = 9.6, 9.3, 8.5, 8.3, 8.1, 7.8−8.0, 7.6, 7.4−7.5, 7.29, 7.2, 7.1, 6.85, 6.72, 5.96, 5.76. ^{13}C NMR [DMSO-d_6, 300 MHz]: δ = 169.62, 168.79, 168.32, 160.14, 159.44, 158.12, 156.88, 156.46, 155.51, 150.96, 150.78, 149.91, 148.45, 147.67, 147.23, 140.87, 139.45 (two signals are merged), 136.97, 136.15, 135.16, 128.16, 126.65 (two signals are merged), 125.08, 124.20, 123.64, 123.43 (two signals are merged), 122.49, 120.22, 119.13, 118.73.

Synthesis of Na[Co(L^2)$_2$−($ZnCl_2$)$_2$] (4). This compound was synthesized following the procedure of **3** with the following reagents: Na[Co(**2**)$_2$] (**2**) (0.100 g, 0.14 mmol), $ZnCl_2$ (0.080 g, 0.59 mmol), and DMF (10 cm^3). After stirring the reaction mixture for 1 h, the filtrate was subjected to diethyl ether diffusion. This afforded the deep-yellow crystalline compound within 2 days. Yield: 0.040 g (50%). Anal. Calcd for $C_{34}H_{22}N_{10}O_4Cl_4NaCoZn_2$: C, 41.29; H, 2.24; N, 14.16. Found: C, 41.40; H, 2.55; N, 14.28. IR (KBr, selected peaks, C═O): 1646, 1601, 1557 cm^{-1}. Conductivity (~1 mM solution at 298 K): Λ_M = 10 (in CH_3CN), 60 (in DMF) Ω^{-1} cm^2 mol^{-1}. Absorption spectra [λ_{max}, nm, DMF (ϵ, M^{-1} cm^{-1})]: 658 (160), 504 (sh, 800), 470 (sh, 2090), 425 nm (sh, 3340). ES-MS (H_2O, *m*/*z*): Obsd 895.3060 (30) [{$Co(L^2)_2$-$(ZnCl)_2$}$^+$] Calcd 894.81. ^{1}H NMR [DMSO-d_6, 300 MHz]: δ = 7.87 (d, 4H, br, $H_2/H_{2'}$), ~7.1 (m, 4H, br, $H_3/H_{3'}$), 7.57 (m, 4H, br, $H_4/H_{4'}$), 7.70 (d, 4H, $H_5/H_{5'}$), 6.94 (d, 4H, $H_9/H_{9'}$), 8.08 (t, 2H, H_{10}). ^{13}C NMR [DMSO-d_6, 300 MHz]: 148.32 (C_2), 123.02 (C_3), 124.10 (C_4), 120.52 (C_5), 156.08 (C_6), 167.37 (C_7), 158.84 (C_8), 139.31 (C_9), 140.65 (C_{10}).

Synthesis of [Co(L^2)$_2$−($ZnCl_2$){Zn(Cl)(DMA)}] (4a). When the reaction for the synthesis of **4** was performed in DMA, complex **4a** was isolated instead. Yield: 0.085 g (60%). Anal. Calcd for $C_{38}H_{33}N_{11}O_6Cl_3CoZn_2\cdot H_2O$: C, 44.06; H, 3.21; N, 14.87; Cl, 10.27. Found: C, 43.64; H, 3.44; N, 14.87; Cl, 10.02. IR (KBr, selected peaks, C═O): 1640, 1601, 1560 cm^{-1}. Conductivity (DMA, ~1 mM solution at 298 K): Λ_M = 2 Ω^{-1} cm^2 mol^{-1}. Absorption spectra [λ_{max}, nm, DMA (ϵ, M^{-1} cm^{-1})]: 658 (100), 474 (sh, 1800), 412 nm (sh, 4580). ES-MS (DMSO, *m*/*z*): Obsd 894.0370 (30) [{$Co(L^2)_2(ZnCl)_2$}$^+$] Calcd 894.08. ^{1}H NMR [DMSO-d_6, 300 MHz]: δ = 8.03 (d, 4H, br, $H_2/H_{2'}$), ~7.1 (m, 4H, br, $H_3/H_{3'}$), 7.6 (m, 4H, br, $H_4/H_{4'}$), 7.75 (d, 4H, $H_5/H_{5'}$), 7.02 (d, 4H, $H_9/H_{9'}$), 8.1 (t, 2H, H_{10}), 2.97 (CH_3, DMA), 2.81 (CH_3, DMA), 1.98 (CH_3, DMA).

Synthesis of [Co(L^2)$_2$−($ZnCl_2$){Zn(Cl)(DMF)}] (4b). This was synthesized using DMF in a manner similar to that for **4a**. Yield: 0.090 g (64%). Anal. Calcd for $C_{37}H_{31}N_{11}O_6Cl_3CoZn_2\cdot H_2O$: C, 43.49; H, 3.06; N, 15.08. Found: C, 43.24; H, 3.14; N, 14.89. IR (KBr, selected peaks, C═O): 1646, 1601, 1557 cm^{-1}. Conductivity (DMF, ~1 mM solution at 298 K): Λ_M = 0 Ω^{-1} cm^2 mol^{-1}. Absorption spectra [λ_{max}, nm, DMF (ϵ, M^{-1} cm^{-1})]: 658 (160), 504 (sh, 800), 470 (sh, 2090), 425 nm (sh, 3340). ^{1}H NMR [DMSO-d_6, 300 MHz]: δ = 8.06 (d, 4H, br, $H_2/H_{2'}$), 7.06 (m, 4H, br, $H_3/H_{3'}$), 7.57 (m, 4H, br, $H_4/H_{4'}$), 7.72 (d, 4H, $H_5/H_{5'}$), 7.06 (d, 4H, $H_9/H_{9'}$), 8.05 (t, 2H, H_{10}), 2.94 (CH_3, DMF), 2.77 (CH_3, DMF), 7.96 (CHO, DMF).

General Procedure for the Beckmann Rearrangement Reaction. To a solution of complex **4b** (0.017 g, 0.018 mmol) in DMF (3 mL) was added a DMF solution (2 mL) of acetophenone oxime (0.050 g, 0.36 mmol), and the resultant solution was stirred at 100 °C for 2 h over an oil bath. The progress of the reaction was monitored by thin-layer chromatography using a mixture of hexanes−ethyl acetate (8:2). The solvent was removed under reduced pressure, and the organic products were extracted with ethyl acetate. The organic products were purified by column chromatography, while the metal complex was washed with diethyl ether, dried under vacuum, and was suitable for reuse.

Physical Measurements. The conductivity measurements were done in organic solvents or water using the digital conductivity bridge from Popular Traders, India (Model No. PT-825). The elemental analysis data were obtained from an Elemental Analysensysteme GmbH Vario EL-III instrument. The NMR measurements were done using an Avance Bruker (300 MHz) instrument. The infrared spectra (either as KBr pellet or as a mull in mineral oil) were recorded using a Perkin-Elmer FTIR 2000 spectrometer. The absorption spectra were recorded using a Perkin-Elmer Lambda-25 spectrophotometer. The mass spectra were obtained on a JEOL SX102/DA-6000 instrument. The thermal analyses were performed with a Shimadzu DTG-60 instrument in the temperature range 25−800 °C.

Crystallography. Single crystals suitable for X-ray diffraction studies were grown by the vapor diffusion of diethyl ether to a DMF, CH_3CN, or DMA solution of the compound, having the following compositions: **1**·DMF, **2a**·H_2O, **3**·CH_3CN, and **4a**·2DMA. The suitable crystals of **1**, **2a**, **3**, and **4a** were mounted lengthways with the largest dimension in a sealed capillary filled with respective mother liquor solution. The intensity data were collected on a Bruker AXS SMART-APEX CCD diffractometer equipped with a molybdenum sealed tube (Mo Kα = 0.710 73 Å) and a highly orientated graphite monochromator.[31] Frames were collected at T = 298 K (100 K for **1**) by ω, ϕ, and 2θ rotation at 10 s per frame with SMART.[31] The measured intensities were reduced to F^2 and corrected for absorption with SADABS.[32] Structure solution, refinement, and data output were carried out with SHELXTL,[33] and structures were solved by a direct method. Non-hydrogen atoms were refined anisotropically by the full-matrix least-squares method, while the hydrogen atoms were constrained by a rigid model. Hydrogen atoms for an asymmetric water molecule in **2a** could not be located from the difference Fourier map. Table 1 contains necessary crystallographic details.

CCDC 622540−622543 contain the supplementary crystallographic data for this paper. These data can be obtained free of charge from the Cambridge Crystallographic Data Center via www.ccdc.cam.ac.uk/data_request/cif.

Acknowledgment. R.G. is thankful for the generous financial support from the Department of Science and Technology (DST), New Delhi, crystallographic help received from IIT−Delhi (Prof. A. Ramanan and Prof. A. K. Ganguli), IIT−Kanpur (Prof. P. K. Bharadwaj), DST−FIST funded single-crystal diffraction facility at IIT−Delhi for the data collection of a few samples, and the DST−FIST funded MS facility at this department.

Supporting Information Available: Figures for crystal structure of molecule **B** of complex **2a** (S1), absorption spectra (S2), ^{1}H and ^{13}C NMR spectra (S3−S6), and thermal studies (S7) and Table S1 containing bonding parameters and a CIF file. This material is available free of charge via the Internet at http://pubs.acs.org.

IC7016424

(31) *SMART: Bruker Molecular Analysis Research Tool*, version 5.0 618; Bruker Analytical X-ray Systems, 2000.
(32) *SAINT-NT*, version 6.04; Bruker Analytical X-ray Systems, 2001.
(33) *SHELXTL-NT*, version 6.10; Bruker Analytical X-ray Systems, 2000.